

## STUDY ON BIODIESEL HEAT TRANSFER THROUGH SELF-TEMPERATURE LIMIT INJECTOR DURING VEHICLE COLD START

by

**Jun WANG<sup>a</sup>, Yan KANG<sup>b\*</sup>, Lin YANG<sup>c</sup>, Xiaolu LI<sup>a</sup>, and Tianhong YAN<sup>a</sup>**

<sup>a</sup> College of Mechanical & Electrical Engineering, China Jiliang University, Hangzhou, China

<sup>b</sup> Research Institute of Economic and Social Development,  
Zhejiang University of Finance & Economics, Hangzhou, China

<sup>c</sup> School of Aerospace, Mechanical and Manufacturing Engineering, RMIT University,  
Melbourne, Australia

Original scientific paper

DOI: 10.2298/TSCI141011177W

*A type of self-temperature limit-injector is proposed to reduce the biodiesel consumption and emission in vehicle cold start process. The self-temperature limit-injector is capable of fast raising fuel temperature, which helps improve the quality of diesel spray and its combustion efficiency. A self-temperature limit-injector model is established with consideration of electro-mechanic coupling and fluid-structure interaction. A transient simulation is conducted using dynamic grid technology. The results show that self-temperature limit-injector can effectively raise biodiesel temperature to 350K from 300K in 32 seconds. That is to say, adding self-temperature limit-injector to existing biodiesel combustion system is an environment-friendly solution due to improving atomization and spray quality quickly.*

Key words: *injector, dynamic grid, biodiesel, emission, heat transfer*

### Introduction

With the continuous development of world economy, the petroleum resource is getting scarcity. Automobile powered by internal combustion engine consumes a large amount of petroleum resource and produce serious pollution in the meantime. According to the 2010 statistics data from Environment Protection Centers of China, exhaust emissions of automobile counted up to 64% among all the air pollution resources in China [1]. During the vehicle cold start process, hydrocarbon (HC), carbon monoxide (CO) emission, and nitrogen oxides (NO<sub>x</sub>) pollution count up to 80% and 50% of all the pollutions, respectively [2]. Therefore, clean and efficient combustion technologies are urgently required in order to release existing environment problems.

The research on biodiesel is getting more popular in recent years [3]. Because the biodiesel raw materials are plenty and its cetane value is sufficient. In addition, biodiesel does not contain aromatic HC and sulfur quantity is of minimum. This is non-toxic and highly biodegrade type of fuel. During the process of biodiesel manufacturing and real applications, production of atmospheric carbon dioxide (CO<sub>2</sub>) is not accumulated. So the greenhouse effect can be mitigated and virtuous circle of ecosystem can be maintained, which make it a truly *green fuel*.

\* Corresponding author; e-mail: wjky163@126.com

In literature of bioethanol blended with diesel, Park *et al.* [4] revealed that some properties blended fuels generally decreased with increased bioethanol content, so the vaporization is easier. By increasing the quantity of engine load, the ignition is quicker and fuel combustion duration is longer. The  $\text{NO}_x$  and indicated specific nitrogen oxides emission increase and CO and HC emission decreases due to the increasing oxygen quantity. In the experiment of burning biodiesel in direct injection engine Z4I02QF, Sun *et al.* [5] suggested that emission of CO, HC, and soot emission of biodiesel is lower than those of traditional diesel, but  $\text{NO}_x$  emission is higher. Johansson *et al.* [6] found that neat biodiesel such as fatty acid methyl ester (FAME), soybean methyl ester, and rapeseed methyl ester can effectively decrease soot emission even when blending with traditional diesel in a lower ratio. However,  $\text{NO}_x$  emission is numerous because of high flame temperature. This study suggests FAME and diesel-blended FAME can be potential solutions to fulfill the requirements of future emission legislation in terms of vehicle exhaust gas emission. Low soot emission and correspondingly low  $\text{NO}_x$  emission can be achieved because of renewable FAME fuel which has lower impact on global warming compared with burning diesel. Wagner *et al.* [7] studied effects of methyl ester, ethyl ester, and butyl ester of soybean oil on engine performance and exhaust emission. Results shows that quantity of exhaust emission such as HC, CO, and particulate matter (PM) exerted minor change no matter what kind of fuels was used, but  $\text{NO}_x$  emission is generally elevated in every case. In the situation of fully loading the engine, soot decreases when using methyl ester and ethyl ester but increases when using butyl ester. Another study from Park *et al.* [8] indicates that biodiesel generate lower  $\text{NO}_x$ , soot, CO, and HC emission compared with traditional diesel with same injection quantity. Nouredini *et al.* [9] found that two different types of methyl ester derived from rapeseed oil could significantly reduce the emission of total PM and aromatic hydrocarbon, but increase emission of  $\text{NO}_x$  and formaldehyde in the meantime. Sharps *et al.* [10] and Sharps [11] researched biodiesel emission characteristics in Diesel engine. Their conclusion is that biodiesel can significantly reduce PM emission. Staat and Gateau *et al.* [12] studied power emission performance of biodiesel produced by rapeseed oil in Diesel engine. They have tracked the performance of biodiesel applied in Diesel engine for three years. The results indicate that using biodiesel can reduce HC and PM emission, but  $\text{NO}_x$  production is elevated. Besides, the application of B30 can significantly reduce HC emission, but quantity of aldehyde emission barely changes. Results of various studies indicate the fact that the application of biodiesel could effectively improve combustion and reduce emission of soot, HC, and CO when comparing with tradition diesel burning in same engine conditions, while  $\text{NO}_x$  emission exerts only a slight growth.

In order to improve combustion and reduce emission during cold start, scholars have studied characteristics of spray and atomization of fuel. Changsik *et al.* [13] proposed an innovative concept which simulates the behavior of the multi-component fuel spray impinging on a hot surface. They reach the conclusion that the distribution of vapor mass depends on the volatility of the fuel spray, and the increased degree of superheat between the hot wall surface temperature and the spray droplet temperature results in the increase of fuel vapor mass in the impinged spray. Topladi *et al.* [14] introduced a more advanced spray model which can predict spray, combustion, and exhaust emission. Harun *et al.* [15] developed a mechanism of reduced-chemical kinetics. It is proved to be reliable in predicting in-cylinder combustion and emission after being compared with results of other CFD algorithms. Yamazaki *et al.* [16] studied atomization characteristics of superheated fuel and found that atomization performance can be improved by increasing fuel temperature. Hyung *et al.* [17] presented a method to reduce emission in dimethyleter (DME) fueled Diesel engine by optimizing injection time. Zhang *et al.* [18] explored the effect of atomization of superheated fuel on combustion and emission based in a Die-

sel engine of swirl chamber. Research results revealed that fuel consumption and the quantity of main emissions decreased within certain temperature range. Huang *et al.* [19, 20] raised a concept about atomization behavior of fuel containing dissolved gas and recirculation of internal exhaust gas of spray. In the high pressure circumstance, CO<sub>2</sub> is firstly dissolved into fuel. Fuel is then injected into the engine cylinder. Atomization effect is improved eventually. Meanwhile, NO<sub>x</sub> emission is reduced owing to the internal exhaust gas recirculation effect of CO<sub>2</sub>. Zhang *et al.* [21] presented a highly dispersed spray nozzle model and drew a conclusion that engine equipped with new nozzle has a lower emission level and better brake special fuel consumption performance. Senda *et al.* [22] proposed a model of fuel atomization and evaporation. It can calculate spray parameters such as particle diameter tallied from test results.

In general, fuel atomization can improve the performance of engine cold start, combustion and emissions [23-26].

In consideration of mentioned studies, it is obvious that research on fuel heat transfer in injector during vehicle cold start is an important topic in term of improving combustion technology.

### **The relevant theories and modeling of heat transfer and fluid for self-temperature limit-injector**

Compared to general fuel injector, a more complex heat transfer process in self-temperature limit-injector (STL-injector) will occur. Hence some significant phenomenon of fuel spray and atomization outside the injector outlet could be observed. In this chapter, the STL-injector calculation model and reveal relevant theories will be established.

#### ***Study on heat transfer of STL-injector***

##### *Positive temperature coefficient (PTC) intelligent heating materials*

The PTC material is a kind of resistor whose resistance positive correlate with its temperature. The resistance change is small within a certain temperature range. When the temperature exceeds a certain value (named as Curie point), its resistance increases rapidly with scale between 10<sup>3</sup> and 10<sup>9</sup>, which close to the insulator [27].

Different Curie point can be obtained by using different PTC material. The PTC is powered by electricity, and its heating power will decline with the rise of its temperature. The fuel embedded by PTC material can be maintained at a higher temperature. So the *smart heated* fuel may be realized to improve atomization and spray during the engine's cold start.

##### *The STL-injector work mechanism*

This research proposes a kind of method to heat fuel in injector based on PTC material, which can reduce the fuel viscosity, improve engine cold start performance. The PTC material embedded in injector can heat fuel controllably by utilizing its temperature-resistance characteristics. Thus the fuel can be ensured not to exceed the boiling point to avoid generating phase change in injector during engine cold start. So it can be named as STL-injector.

Narrow space, fast-changing and high-pressure turbulent fluid as well as slow heat transfer, makes research more challenge, and these problems have been compromised in order to achieving study aims.

The fuel in STL-injector can be heated quickly by using vehicle battery. Ideally, fuel viscosity can be reduced, atomization and spray quality can be better, and combustion efficiency is improved. Thus emissions can be reduced during engine cold start, the goals of saving energy and reduction emission can be achieved. The STL-injector model is established as shown in fig. 1.,

where the fig. 1(a) is longitudinal view of STL-injector and the fig.1(b) is enlarged view of nozzle. The brown segment of sub fig. 1(a) and sub fig. 1(b) represent shell and needle valve. The yellow segment means fuel and the red stands for the PTC heating material. The PTC material embedded pipe can be seen at the upper section of STL-injector. At the lower section, PTC material is respectively embedded in the injector exterior and bottom of STL-injector. Point number 1 to 4 are analysis points for calculated temperature of the model.

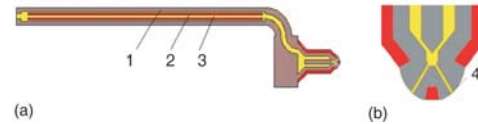


Figure 1. The STL-injector calculation model

Because the fuel in injector is a transient and high-pressed fluid, relevant experimental and theoretical studies need to be done to understand atomization of biodiesel. The impact factors include flow, heat transfer in STL-injector. Atomization and spray characteristics of fuel are affected by the performance of the PTC material, while engine combustion and emissions are subsequently affected by atomization and spray. Aims of this research are to establish and calculate heat transfer of STL-injector model for appraising its effects to biodiesel during engine cold start.

In this model, the upper parts of STL-injector are not taken into consideration because it is supposed that heat transfer can be ignored here. Meanwhile, due to the calculation cost of 3-D model (including time and equipment) and grid technology, 3-D model is hard to achieve computational requirements. Therefore, a 2-D model is chosen in this work. The grid structure of model main parts is shown in fig. 2.

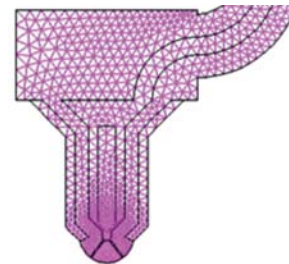


Figure 2. The 2-D grid of STL-injector

### Heat transfer characteristics in STL-injector during engine cold start

Heat transfer of flow field inside STL-injector is very slow. But on the contrary, the high frequency characteristics of pressure and velocity make analysis difficult. Also resistance of PTC material changes with temperature. Therefore, the transient heat transfer in the flow field forms a large-scale, two-stage automatic feedback system during cold start. Block diagram is shown in fig. 3.

Among them,  $P_t$  which determines electrical resistance of material is surface temperature of PTC. The  $W_{ti}$  is the wall temperature (wall heat transfer,  $t$  represents temperature and  $i$  means respective point of the wall). The  $F_{tj}$  means fuel temperature ( $j$  is respective point of flow field). The  $B_t$  is the fuel temperature in bank (the initial fuel temperature is constant, but the amount of fuel pressed into injector changes according to jet rule) and  $Z_t$  is nozzle temperature.

Fuel enters into STL-injector which powered by an on-board power supply during cold start. The resistance of PTC materials is very small in the beginning, so the electrical energy is rapidly converted into heat energy and transfer to the surrounding devices and fuel. In the process of heat transfer, resistance of PTC material keeps changing with PTC temperature variation. Resistance increases quickly up to thousands of times of the original value when PTC tem-

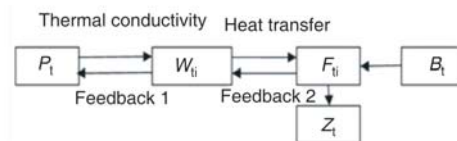


Figure 3. Transient heat transfer schematic diagram of STL-injector during cold start

perature is around the Curie point. The output power of PTC decreases correspondingly. At the same time, the velocity and pressure at the input and output of STL-injector change with certain laws, so the STL-injector is a automatic control system with two level feedback and the first level needs to be controlled artificially. In this research, a heat transfer model will be built and parameterized. Eventually, heat transfer characteristics under complex working circumstance will be revealed.

### **Transient study on heat transfer of STL-injector**

In STL-injector, the heat transfer and flow depends on time need deal with some questions such as thermo-solid coupling and fluid-structure interaction. In solid, thermal conductivity is the predominate way in heat transfer. Heat transfer is governed by Navier-Stokes equations in fluid.

#### *Thermal conductivity of solid*

The PTC material powered by vehicle battery provides heat for fuel in STL-injector. This heating source names source terms. The heat power may be calculated by eq. (1):

$$P = \frac{U^2}{R(\text{temp})} \quad (1)$$

Among the equation,  $P$  is the heating power of the PTC material,  $U$  – the battery voltage, and  $R(\text{temp})$  – the resistance of the PTC material, which depends on its temperature.

The simulation software can read system temperature with user define function (UDF) written by macro function of CFD tools. Combined with the temperature-resistance characteristics of PTC materials chosen in work, it can get correspondent heating power varied with temperature of PTC material. The temperature-resistance curve of PTC materials whose Curious point is 130 °C, was chosen in this work and shown in fig. 4.

It can be seen from fig. 4, the resistance of PTC material continuously varies with temperature, and the output power of PTC ceramics changes accordingly. The heat resource terms can not be set-up as a constant simply. Therefore a UDF is written for resource terms to describe this change.

It is necessary to discuss all the questions about resistance corresponded with temperature. According to eq. (1), the heat power of PTC material can been calculated. But the heat source terms are described with the density of power, so the power density is calculated and return its value back to FLUENT. The power density can be calculated with eq. (2):

$$w = \frac{U^2}{[VR(\text{temp})]} \quad (2)$$

Among them,  $w$  [ $\text{wm}^{-3}$ ] is the power density,  $U$  – the voltage provided with vehicle battery, and here is 24V direct current,  $R(\text{temp})$  [ohm] – the instantaneous resistance of PTC material, and  $V$  [ $\text{m}^3$ ] – the volume of PTC.

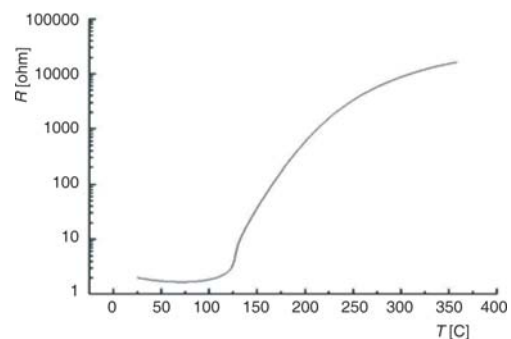


**Figure 4. The temperature-resistance curve of PTC material whose Curious point is 130 °C**

In the solid region, CFD uses energy equation:

$$\frac{\partial}{\partial t}(\rho h) + \nabla(\vec{v}\rho h) = \nabla(k\nabla T) + S_h \quad (3)$$

where  $\rho$  is the density,  $h = \int_{T_{ref}}^T c_p dT$ ,  $k$  – the thermal conductivity,  $T$  – the temperature, and  $S_h$  – the heat source term of volume.

#### *Differential control equation of coupled flow and heat transfer*

Fluid movement is turbulent flow in injector, flow model includes three main differential equations [28, 29], and they are, respectively, describe in eqs. (4)-(7). Besides, we adopt realizable  $k$ - $\varepsilon$  turbulent model for its fine performance in dealing with complex flow conditions.

Mass conservation equation, also known as the continuity equation, is a base of numerical calculation theory of flow and heat transfer:

$$\frac{\partial \rho}{\partial t} + \nabla(\rho \vec{U}) = 0 \quad (4)$$

Momentum conservation equation, also known as Navier-Stokes equation is:

$$\frac{D(\rho \vec{U})}{Dt} = \rho \vec{F} - \nabla p + \mu \Delta \vec{U} \quad (5)$$

Energy conservation equation in terms of the specific total enthalpy is:

$$\frac{\partial(a_L \rho h_{tot})}{\partial t} + \nabla(a_L k_{eff} \nabla T) = \nabla(a_L \tau_{eff} u) + a_L \rho (ug) + \frac{\partial(a_L p)}{\partial t} + S_h \quad (6)$$

where  $\vec{U}$  is the velocity vector,  $\mu$  – the fluid dynamic viscosity,  $h_{tot}$  – the specific total enthalpy is the sum of the specific static enthalpy  $h$ , the flow mean kinetic energy, and the turbulent kinetic energy  $k$ :

$$h_{tot} = h + \frac{uu}{2} + k \quad (7)$$

#### **Boundary conditions configuration**

Influence of fuel injector properties, material properties, thermal boundary conditions, inlet and outlet boundary condition, needle motion, and time step segmentation were investigated.

#### ***Inlet and outlet boundary condition***

In order to obtain the inlet pressure data of STL-injector, an experiment was conducted with biodiesel in the oil pump test bench named LBD 860-075 and powered by electrical motor whose rotation speed is in range of 0-4000 rpm, which made in Zhongyi Labaodi Mechanism Equipment Co. Ltd. We use an ordinary mechanic injector whose opening pressure is 25 MPa to test inlet pressure. The sampling frequency is 100 kHz, the motor speed is approximately 3332 rpm, 1667 rpm, 833 rpm, and 417 rpm, respectively. The oil pump test bench and pressure curve are shown in figs. 5 and 6, respectively. Pressure boundary condition of outlet is set up as a standard atmospheric pressure for two reasons:

- the computer cannot meet the requirement of higher sample frequency for such large-scale computation adopting dynamical grid technology. So, even if a UDF of a real high sampling frequency output pressure data is used, the simulation results would not have any difference in this situation, and

- the key point of our research is heat transfer inside STL-injector, and the fluid temperature in injector is barely impacted by output pressure.

### ***Motion of needle valve and the segment of calculation time***

For the simulation, in one specified time, the position of the needle valve could basically fulfill the experimental requirements. Lift of needle valve is around 0.5 mm. In order to save computing resources, redrawing mesh strategy is an easier way for changing mesh, meanwhile it also could maintain good meshing quality. It is noteworthy that it is more important to consider the real time position of the needle valve than how it arrives there. Because of the dispersion of numerical calculation, maintaining a constant speed at every time stamp is expected. As a result, a law restricting speed increment changes within each time stamp is defined in this study. The variation law of lifting speed, time and height is shown in fig. 7.

In fig. 7, the left ascending part describes rising movement law of needle valve for calculation in this paper. The ordinate represents needle speed, while the abscissa represents the time line. In the rising process, needle is restricted by algorithms to be able to sample only once at each speed step and sampling time remained constant. Total rising heights is the shadow area. Similarly, the right step and the shadows represent the needle drop velocity gradient and the height of fall, respectively. One sampling per descendant step is also defined in this process.

Due to the requirements of fidelity of variable sampling signal, computation time consumption will also need to be considered. Sampling time is segmented in this study. After numerous practices, each injection period is decided to be divided into two sub-segments. The first time segment represents a small period before and after needle valve is opened. In this period, the sampling frequency is set-up in unit of MHz. The other time segment takes only one time step in this work.

### ***Material properties and heat transfer boundary setting***

In this work, the viscosity of biodiesel is taken from the literature [30]. The data curve diagram is shown in fig. 8. Here as a reference, the 0# diesel is a kind of diesel according to diesel classification standard in China.



Figure 5. Oil pump test bench

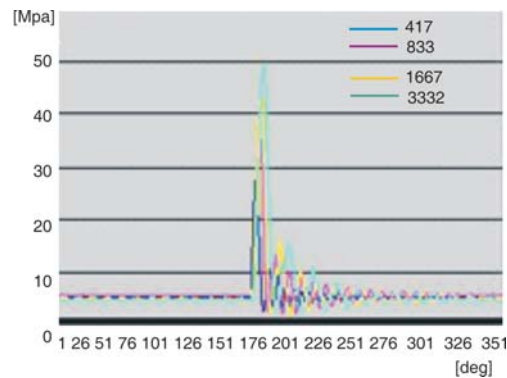


Figure 6. Pressure curve of high pressure inlet of injector under different speeds

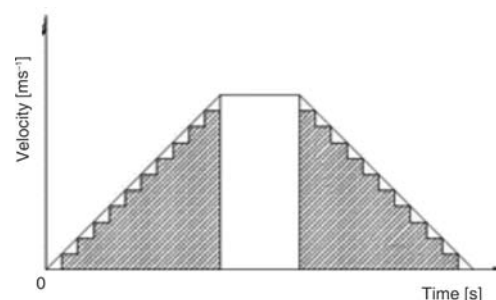


Figure 7. Diagrammatic sketch for time and position of needle rise and fall

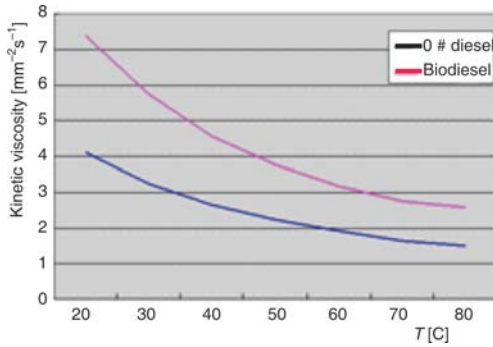


Figure 8. Biodiesel viscosity curves

Table 1. Biodiesel thermal conductivity

Temperature [K]	300	400	500	600	700
Thermal conductivity [Wm <sup>-1</sup> k <sup>-1</sup> ]	0.175	0.16	0.14	0.12	0.09

Table 2. Solid material properties [27]

	PTC	Injector
Density [kgm <sup>-3</sup> ]	5600	8030
Specific heat capacity $c_p$ [Jkg <sup>-1</sup> k <sup>-1</sup> ]	545	502.48
Thermal conductivity [Wm <sup>-1</sup> k <sup>-1</sup> ]	0.9156	16.27
Heat dissipation coefficient $D^*$ [mwk <sup>-1</sup> ]	10-15	
Molecular weight [kgkg <sup>-1</sup> mol <sup>-1</sup> ]	180	

Table 3. The specific heat capacity of biodiesel

Temperature [K]	298.15	308.15	318.15	328.15
Specific heat capacity [Jkg <sup>-1</sup> k <sup>-1</sup> ]	2762	2867	2992	3101

state, 834 rpm. Fuel type, biodiesel backpressure, 1 standard atmosphere. Fuel flow simulation time, 32.544 seconds. After CFD simulation, the temperature contours of four moments are shown in figs. 9-12. After 32.544 seconds, the average outlet temperature of biodiesel from STL-injector is 352 K.

It can be seen from figures that temperature ascends very fast in STL-injector body but has only a slow increase in fuel. It means functions of STL-injector have prodigious potential to be improved if fuel can be heated more quickly. It can be found that fuel temperature rises more slowly near the nozzle and in the oil chamber than in the upper segment. Therefore, the key is to

Thermal conductivity of biodiesel derived from estimation by Li [31]. Value is shown in tab. 1.

Table 2 is physical properties of PTC material and shell material of STL-injector.

Density of biodiesel employs an improved expression of Yamada and Gunn [32] based Rackett [33] eqs.

$$\rho = \rho^r (0.29056 - 0.08775\omega)^{-\phi} \quad (8)$$

Among them,  $\rho$  [gcm<sup>-3</sup>] is the biodiesel's density depended on temperature, and  $\rho^r$  – the reference density. Here  $\rho^r = 871.5$  g/cm<sup>3</sup> [30], and  $\phi$  – the temperature coefficient, whose value depended on temperature complies with the equation:

$$\phi = \left(1 - \frac{T}{T_c}\right)^{\frac{2}{7}} - \left(1 - \frac{T^r}{T_c}\right)^{\frac{2}{7}} \quad (9)$$

where  $T_c$  [K] is the critical temperature,  $T^r$  [K] – the reference temperature corresponding to the reference density  $\rho^r$ . Other parameters, such as the eccentricity factor, critical pressure, critical volume represent [34]:  $\omega_m = 0.694$ ,  $T_{cm} = 798.5$  K,  $p_{cm} = 14.21$  bar,  $V_{cm} = 1\,082.09$  cm<sup>3</sup>/mol, respectively.

Based on these formula and parameters, density of biodiesel can be prepared into UDF file. According to [35]. Specific heat capacity of biodiesel is listed in tab. 3.

### Calculation results and comments

The CFD simulation of STL-injector operation process is based on the following conditions. Curie temperature of PTC material, 403 K. Inlet fuel temperature, 300 K. Engine operation



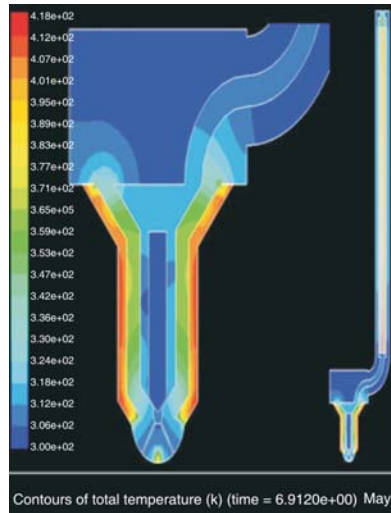


Figure 9. The STL-injector temperature mapping,  $t = 6.612$  s

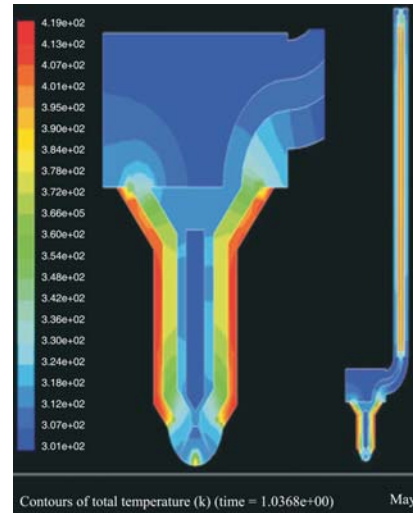


Figure 10. The STL-injector temperature mapping,  $t = 10.368$  s

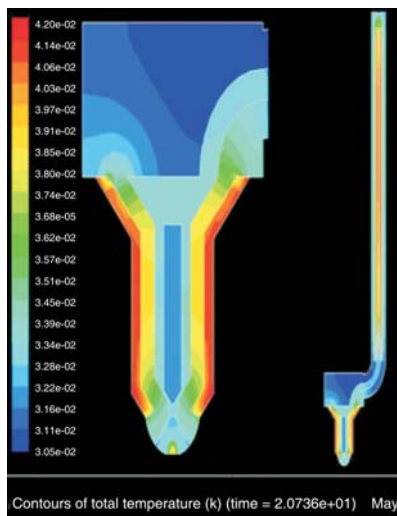


Figure 11. The STL-injector temperature mapping,  $t = 20.736$  s

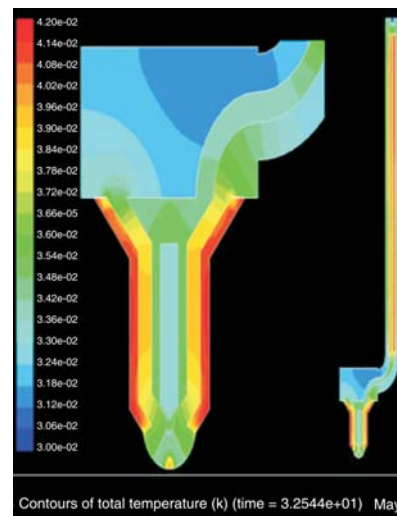


Figure 12. The STL-injector temperature mapping,  $t = 32.544$  s,

improve the design of nearby nozzle and oil chamber. Besides, the use of high-voltage current source and PTC with higher Curious point will be tested.

Energy-saving and emission reduction are long-term challenges for automotive industries. Study on combustion mechanism and searching for alternative types of fuel have important theoretical and practical values. Based on the knowledge that atomization can be further improved by heating fuel, improving combustion, and reducing emission, a new fuel injector

model has been proposed in this research. The CFD tools have been employed to analyze transient heat transfer of this model. The research focus locates on the thermal physical state of biodiesel injection which is affected by the combined factors including needle movement, non-linear heat sources and turbulent flow. Some characteristics of temperature variation in injector have been obtained. The calculation results show that biodiesel temperature at injector nozzle increases from 300K to 352 K in 32.544 seconds. It suggests that the STL-injector can effectively reduce biodiesel viscosity during engine cold start. This is a precious opportunity to improve biodiesel combustion efficiency and reduce exhaust emission meanwhile.

### Conclusions

According to the calculated results, following conclusions could be obtained:

- the temperature of biodiesel heated 30 seconds inside STL-injector can rise more than 50 degrees, which can improve the effect of fuel atomization, and
- the STL-injector which can effectively improves fuel temperature, is an effective method of saving energy and reducing emission.

### Acknowledgments

The research presented in this paper are supported by Zhejiang Province Nature Science Foundation (LY14E050023, Y1110666 & LQ16D010003), Natural Science Foundation of China (51379198), educates for State Key Laboratory of Satellite Ocean Environment Dynamics (soed1404), and Key Laboratory of Power Machinery and Engineering of Ministry of Education in Shanghai Jiaotong University (2012-5).

### Nomenclature

$c_p$	– specific heat capacity, 1000 [Jkg <sup>-1</sup> K <sup>-1</sup> ]
$g$	– gravity acceleration, [ms <sup>-2</sup> ]
$h$	– enthalpy, [Jkg <sup>-1</sup> ]
$P$	– heating power of the PTC material
$p_{cm}$	– critical pressure, [bar]
$r$	– electrical resistance, [ohm]
$S_h$	– heat source term of volume, [Wm <sup>-3</sup> ]
$T$	– temperature, [K]
$T_c$	– critical temperature, [K]
$T^r$	– reference temperature, [K]
$T_{cm}$	– critical temperature, [K]
$t$	– time, [s]
$U$	– battery voltage, 24 V direct current
$\bar{U}$	– velocity, [ms <sup>-1</sup> ]
$V$	– volume of PTC, [m <sup>3</sup> ]
$V_{cm}$	– critical volume, [m <sup>3</sup> ]

$w$	– power density, [wm <sup>-3</sup> ]
-----	--------------------------------------

#### Greeks symbols

$\mu$	– dynamic viscosity, [kgm <sup>-1</sup> s <sup>-1</sup> ]
$\rho$	– density, [kgm <sup>-3</sup> ]
$\phi$	– temperature coefficient
$\rho^r$	– reference density, [gcm <sup>-3</sup> ]
$\omega_m$	– eccentricity factor

#### Superscript

$r$	– reference value
-----	-------------------

#### Subscripts

eff	– effective
L	– liquid
tot	– total

### References

- [1] Zhang, P., Research on the Numerical Simulation and Experiments of Dimethyl Ether Flash Boiling Spray, Ph. D. thesis, Huazhong Univ. of Sci. & Tec., Wuhan, China, 2009
- [2] Jiang, S. S., et al., Test and Evaluation for Cold-Start Performance of Internal Combustion Engines, *Internal Combustion Engines*, 5 (2003), 1, pp. 53-58
- [3] Cai, Y., et al., Experimental Study on Biodiesel Engine Emissions Using Non-Thermal Plasma, *China Mechanical Engineering*, 19 (2008), 18, pp. 2260-2263
- [4] Park, S. H., et al., Effect of Bioethanol Blended Diesel Fuel and Engine Load on Spray, Combustion, and Emissions Characteristics in a Compression Ignition Engine, *Energy Fuels*, 26 (2012), 8, pp. 5135-5145
- [5] Sun, P., et al., Study of Emission Property of DI-CI Engine Fueled with Biodiesel, *Journal of Agricultural Mechanization Research*, 3 (2006), 3, pp. 209-211

- [6] Johansson, M., et al., NO<sub>x</sub> and Soot Emissions Trends for RME, SME and PME Fuels Using Engine and Spray Experiments in Combination with Simulations, *Fuel*, 106 (2013), 6, pp. 293-302
- [7] Wagner, L. E., et al., Effect of Soybean Oil Esters on the Performance, Lubricating Oil, and Water of Diesel Engines, No. 8413852, SAE Technical Paper, 1984
- [8] Park, S. H., et al., Fuel Spray and Exhaust Emission Characteristics of an Undiluted Soybean Oil Methyl Ester in a Diesel Engine, *Energy Fuels*, 24 (2010), 24, pp. 6172-6178
- [9] Nouredini, H., et al., Immobilized Pseudomonas Cepacia Lipase for Biodiesel Fuel Production from Soybean Oil, *Bioresour Technology*, 96 (2005), 7, pp. 769-777
- [10] Sharps, C. A., et al., The Effect of Biodiesel Fuels on Transient Emissions from Modern Diesel Engines, Part I Regulated Emissions and Performance, SAE paper 2000-01-1967, 2000
- [11] Sharps, C. A., Transient Emissions Testing of Biodiesel and other Additives in a DDC Series 60 Engine, Final Report, National Biodiesel Board, Jefferson City, Mo., USA, 1994
- [12] Staat, F., Gateau, P., The Effects of Rapeseed Oil Menthyl Ester on Diesel Engine Performance, Exhaust Emissions and Long-Term Behavior: A Summary of Three Years of Experimentation, SAE paper 950053, 1995
- [13] Changsik, L., et al., A Study on the Spray & Wall Interaction Model Considering Degree of Superheat in the Wall Surface, *Numerical Heat Transfer, Part B: Fundamentals: An International Journal of Computation and Methodology*, 40 (2001), 6, pp. 495-513
- [14] Topladi, A. K., et al., An Advanced Spray Model for Application to the Prediction of Gas Turbine Combustor Flow Fields, *Numerical Heat Transfer, Part A*, 38 (2000), 4, pp. 325-340
- [15] Harun, Md. I., et al., Development of a Reduced Biodiesel Combustion Kinetics Mechanism for CFD Modelling of a Light-Duty Diesel Engine, *Fuel*, 106 (2013), April, pp. 388-400
- [16] Yamazaki, N., et al., The Effects of Flash Boiling Fuel Injection on Spray Characteristics, Combustion, and Engine Performance in DI and IDI Diesel Engines, SAE paper, 850071, 1985
- [17] Hyung, J. K., et al., A Study on the Reduction of Exhaust Emissions through HCCI Combustion by Using a Narrow Spray Angle and Advanced Injection Timing in a DME Engine, *Fuel Processing Technology*, 92 (2011), 8, pp. 1756-1763
- [18] Zhang, Y., et al., Application Research and Theory Exploration of Fuel Heat Strength in Diesel Engine of Swirl Chamber, *Small Internal Combustion Engine and Motorcycle*, 6 (1993), 6, pp. 25-28
- [19] Huang, Z., et al., Atomization Behavior of Fuel Containing Dissolved Gas, *Journal of Atomization and Sprays*, 41 (1994), 3, pp. 253-262
- [20] Huang, Z., et al., New Concept of Atomization Behavior of Fuel Containing Dissolved Gas, *Journal of Shanghai Jiaotong Univ.*, 28 (1994), 2, pp. 1-6
- [21] Zhang, G., et al., Effects of Highly Dispersed Spray Nozzle on Fuel Injection Characteristics and Emissions of Heavy-Duty Diesel Engine, *Fuel*, 102 (2012), 6, pp. 666-673
- [22] Senda, J., et al., Modeling of Atomization Process in Flash Boiling Spray, SAE paper 941925, 1994
- [23] Frank, Z., et al., An Internally Heated Tip Injector to Reduce HC Emissions During Cold-Start, SAE paper, 1999-01-0792, 1999
- [24] Masaru, K., et al., A Study of the Influence of Fuel Temperature on Emission Characteristics and Engine Performance of Compression Ignition Engine, SAE paper 2002-32-1777, 2002
- [25] Kenjiro, N., et al., Effects of High-Temperature Fuel on In-Cylinder Fuel Mixture Formation Process for Direct Injection Engine, SAE paper 2003-32-0003, 2003
- [26] Seoksu, M., et al., The Effects of Injector Temperature on Spray and Combustion Characteristics in a Single Cylinder DISI Engine, SAE paper 2005-01-0101, 2005
- [27] Zhu, B., et al., PTC Ceramic Manufacture Processing and Properties, Publication of Shanghai University, Shanghai, China, 2001
- [28] Tao, W., Numerical Theory of Heat Transfer, Publ. of Xian Jiaotong Univ., Xian, China, 2004
- [29] George, S., et al., Transient Heating Effects in High Pressure Diesel Injector Nozzles, *International Journal of Heat and Fluid Flow*, 51 (2015), Feb., pp. 257-267
- [30] Zhou, C., Experimental Study of Direct Injection Diesel Engine Perated on High Proportion Biodiesel-DME Blends, Ph. D. thesis, Taiyuan Univ. of Tech., Taiyuan, China, 2008
- [31] Li, Y., Properties Estimation and In-cylinder Working Process Simulation of DME, Biodiesel and the Blend, Ph. D. thesis, Beijing Jiaotong Univ., Beijing, China, 2008
- [32] Yamada, T., Gunn, J., Saturated Liquid Moler Volumes, Rackett Equation, *J. Chem. Eng. Data*, 18 (1973), 2, pp. 234-236
- [33] Rackett, H. G., Equation of State for Saturated Liquids, *J. Chem. Eng. Data*, 15 (1970), 4, pp. 514-517

- [34] Zhao, H., *et al.*, Gas Liquid Property Estimation Manual [v5], Publ. of Chemical Industry, Beijing, China  
[35] Wu, X., *et al.*, The Specific Heat Capacity Measurement of Colza Oil and Biodiesel by Microcalorimeter, *Journal of Engineering Thermophysics*, 28 (2007), 5, pp. 737-740